CHEMISTRY
A European Journal

A Journal of
ChemPubSoc Europe

Accepted Article

Title: Synergetic Metals on Carbocatalyst Shungite

Authors: Martin Pumera

To be cited as: *Chem. Eur. J.* 10.1002/chem.201703974

Link to VoR: http://dx.doi.org/10.1002/chem.201703974

Supported by
ACES

WILEY-VCH

10.1002/chem.201703974

Synergetic Metals on Carbocatalyst Shungite

Rui Gusmão,[1] Zdeněk Sofer,[2] Daniel Bouša,[2] and Martin Pumera[*,1]*

[1]Division of Chemistry & Biological Chemistry, School of Physical Mathematical Science, Nanyang Technological University, Singapore 637371, Singapore

[2]Department of Inorganic Chemistry, University of Chemistry and Technology Prague, Technicka 5, 166 28 Prague 6, Czech Republic.

The natural occurring Palaeoproterozoic carbon mineral shungite is a complex raw carbon microporous matrix, loaded with a wide range of elements. Shungite.exhibits disordered and amorphous structure with highly irregular building blocks. Shungite incorporates metals in its structure, typically catalytic elements such Fe and Ni are also present, as well as, the toxic elements Pb and As at mg/g level. We show here that incorporation of the metals in the carbon matrix of shungite leads into synergiustic catalytic effect. We investigate the application of the shungite in energy related electrochemical catalytic reaction, such as the hydrogen evolution reaction (HER), oxygen evolution reaction (OER) and oxygen reduction reaction (ORR). All elements have a synergetic effect, thus contributing for shungite interesting catalytic performance towards a different range of electrochemical reactions, outperforming other tested carbon allotropes, such as carbon black, metal loaded carbon nanotubes, fullerene and glassy carbon. These findings have profound impact on the application of the natural carbon materials for catalysis.

Keywords: Shungite, Carbon nanomaterials, Metal impurities, oxygen evolution, hydrogen evolution

10.1002/chem.201703974

Introduction

In 1985 a new carbon allotrope, buckminsterfullerene or fullerene,[1] in which the atoms are arranged in closed shells was discovered. Clusters of 60 carbon atoms, C_{60}, were the most abundant, with 20 hexagonal surfaces and 12 pentagonal surfaces. Following initial reports of the detection of naturally occurring fullerenes in some geological samples,[2] specifically shungite triggered both considerable interest and discussion.[3–6]

Precambrian shungite from Karelia (Russia) has an heterogeneous molecular structure in which carbon occurs as 10 nm globules irregularly distributed,[7] with a carbon content from 25% up to 98%.[8] The unusual physicochemical and structural properties of shungite have been used in diverse industrial and environmental applications including water purification and organosynthesis of cyclic hydrocarbons.[9] Interestingly, fullerenes seem only to occur in shungite minerals at very low concentrations (0.1 % wt.).[10]

Shungite was somewhat overlooked when carbon nanotubes (CNT) surpassed fullerenes as the hottest carbon material of the 20th century. Research on CNT was boosted by Iijima in 1991[11] upon the report of their occurrence in the hard deposit growing at the cathode during electric arc experiments to produce fullerenes. Seminal work by Radushkevich and Lukyanovich[12] might nevertheless have been credited for the discovery that carbon filaments could be hollow and have a nanometersize diameter, or what is nowadays known as CNT.[13] Time and time again, the old gives rise to something new. Such was recently the case with graphene, the first established 2D material. Geim and Novoselov isolated graphene in 2004,[14] leading to the 2010 Nobel Prize in Physics. Graphene was obtained from vulgar graphite, which consist upon stacked layer of carbon atoms arranged in sheets of a single atom thick. Each individual sheet is in fact graphene. Nevertheless, its oxidized form has been known since the 19th century.[15] By exposing graphite to strong acids, Brodie obtained a suspension of paper-like foils of graphite oxide, that is, multi-layer staked graphene sheets densely covered with hydroxyl and epoxide groups.

Instigated by the graphene spotlight, new layered materials keep on growing the 2D cluster.[16–19] One of the reasons for the surge of such a wide variety 2D layered materials, is that their electrochemical performance allows for the evaluation of the catalytic activity in view of future applications in energy alternatives, advanced electronic devices and (bio)sensing systems.

Herein we reintroduce shungite, a geological carbon mineral carbocatalyst. Morphological and chemical characterization of this carbon mineral is discussed. The electrochemical

10.1002/chem.201703974

performance in terms of electron transfer is tested in with different carbon allotropes: carbon black (CB), fullerene (C_{60}) and carbon nanotubes (CNT). Energy related applications are evaluated in the hydrogen evolution reaction (HER), oxygen evolution reaction (OER) and oxygen reduction reaction (ORR).

Results and Discussion

Shungite Characterization. The original block is a thick rock of several cm wide, with matt and lackluster appearance, along with greyish opaque lines. The “dull” shungite fragments are known to contain high load of mineral matter.[20] Fragments from a shungite block were grinded for a few seconds using a kitchen blender as detailed in Experimental Section and shown in supplementary information (SI). Powdered and mm fragments of shungite morphology were observed by SEM images, as shown in Figures 1, S1 and S2. In Figure 1a, the mm fragment presents a structure of heterogenous bulk material. Powdered shungite shows (Figure 1b) evidences arrays of micron size crystals, some having a granular structure resembling carbon black (CB) morphology and other suggesting multiple parallel stacked sheets graphite (graphene layers) resulting in irregular thick and several micron lateral size grains. Mapping of elements and EDX spectra of mm size fragment reveals images are shown in Figure S1 and S2. C is the most abundant element as expected, but depending on the area selected, C content varies from 40 to 77%, which is not unusual for shungite samples.[8] Mapping of elements reveals an oxidized surface and an even distribution of Si (19 % max) and a defined stream of S (up to 2%). Other elements detected for different areas were Al and Fe. Other carbon materials were also selected, fullerene (C_{60}) carbon black (CB) and multiwalled carbon nanotubes (CNT) for comparison with shungite. Their characterization is shown in SI.

10.1002/chem.201703974

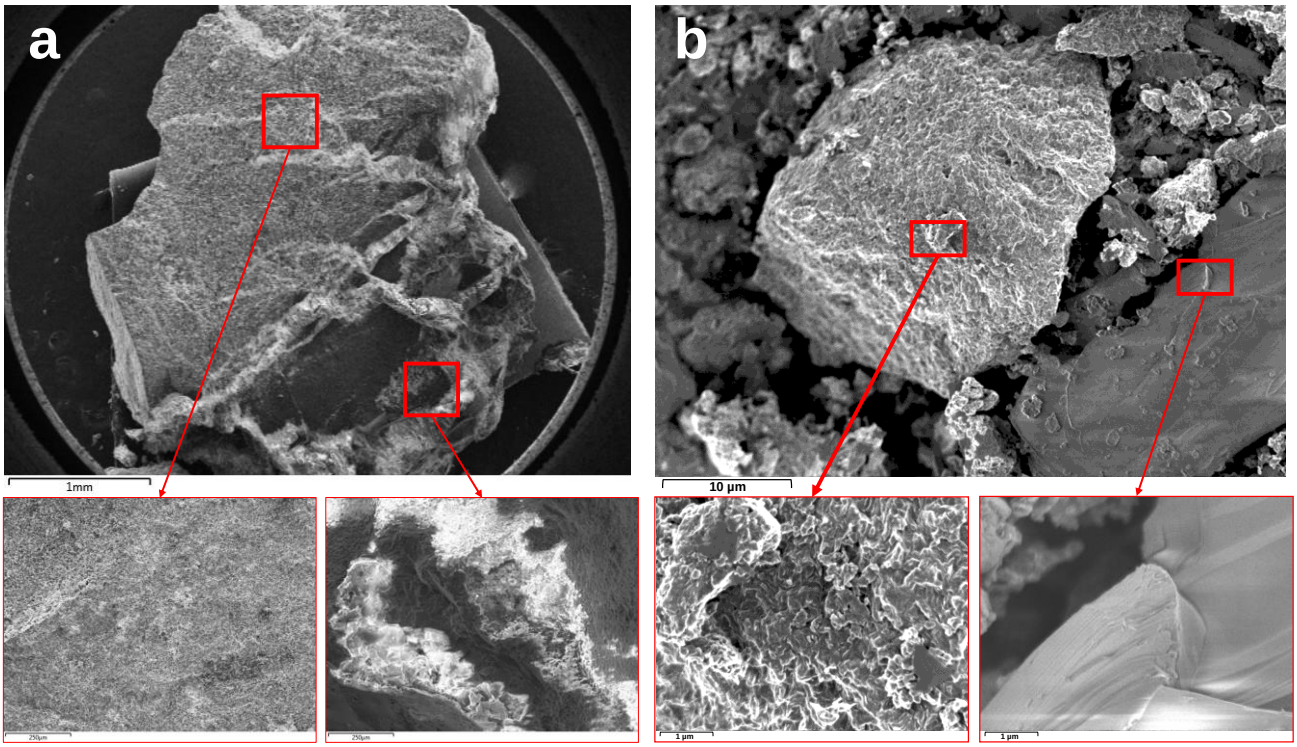

Figure 1. SEM images of a mm size fragment (a) and grinded (b) shungite with amplification of different zones.

Shungite was analyzed by thermogravimetric analysis (TGA) as shown in Figure 2a, which show a stable profile up to 800 ºC under nitrogen atmosphere (~3 % weight loss). This may be assigned to loss of CO and CO_2 molecules by thermal degradation of exposed oxidized surface. Comparison with other carbonaceous nanomaterials is shown on Figure S7. Shungite was also characterized by Raman spectroscopy (Figure 2b) to study structural properties. Pictures were also taken of the acquired spectra area (Figure S8). The D band at approximately 1350 cm^{-1} corresponds to the defects caused by the sp^3-hybridised carbon atoms, while the G band (G from graphite) at approximately 1560 cm^{-1} is related to the sp^2 lattice carbon atoms. The D mode, observed near 1350 cm^{-1}, is a breathing mode of A_{1g} symmetry. The high 1.4 I_D/I_G ratio can be ascribed to a great structural heterogeneity as observed by SEM images and correlate with amorphous-like structure identified by X-ray diffraction.

Photoelectron spectroscopy (XPS) was employed to characterize shungite surface composition as shown in Figure 2c. The peaks of core C 1s and O 1s are visible at energies of 284.4 and 530 eV, respectively. Other elements were also detected (Al 2p, Mg 2s, Si 2p and Sr 3p), coinciding with elements detected by EDS spectra (Figure S1 and S2). Elements

10.1002/chem.201703974

abundance in Table S1 were calculated based on the respective intensities. From these values a 1.9 C/O ratio partial oxidation of shungite, pointing to a partial oxidation of exposed surface.

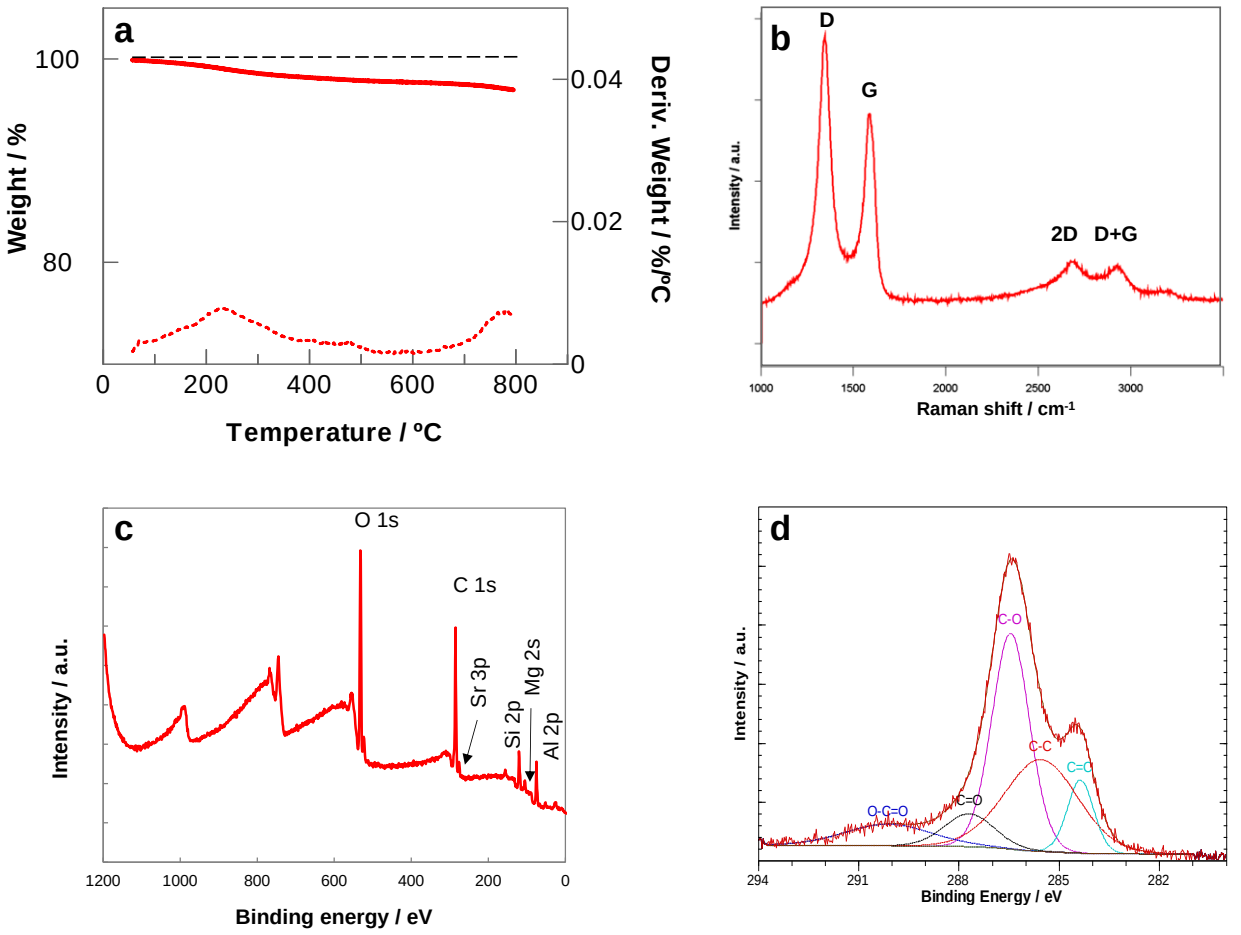

Figure 2. Shungite characterization: a) TGA curves in N_2 flow and respect first derivate b) Raman spectra with an excitation wavelength of 514 nm c) Wide-scan X-ray photoelectron spectra. d) High-resolution X-ray photoelectron spectrum and peaks deconvolution of the C 1s region.

The structure was further investigated by X-ray diffraction showing amorphous-like structure with three broad maxima at 25.5 °2θ, 43.3 °2θ and 78.7 °2θ, which corresponds to 0.348 nm, 0.209 nm and 0.121 nm. The position of maxima are closed to the position of main graphite diffraction pattern, however such large degree of broadening originate from the significant degree of disorder and only short range arrangement of structure. This is in good agreement with the Raman spectroscopy measurement showing high I_D/I_G ratio. Diffractogram is shown on Figure S4.

10.1002/chem.201703974

The structure and distribution of metallic impurities was proofed also by TEM, where can be clearly seen regions with high concentration of metallic impurities. Such accumulations have a dimension in the range of tenths up to hundreds of nanometers. We found in the shungite metallic elements like iron, chromium and vanadium as well as silicon, carbon and chlorine. The localization of iron and oxygen indicate the presence of iron in the form of oxides. The TEM image with corresponding elemental distribution maps are shown on Figure 3a and Figure S5. The TEM images show the amorphous like structure of irregular shungite particles with broad distribution of sizes from micron up to tenths of nanometers. High resolution TEM images show the presence highly disorder layers which is in good agreement with X-ray diffraction data. TEM and HR-TEM images are shown on Figure 3 and S6.

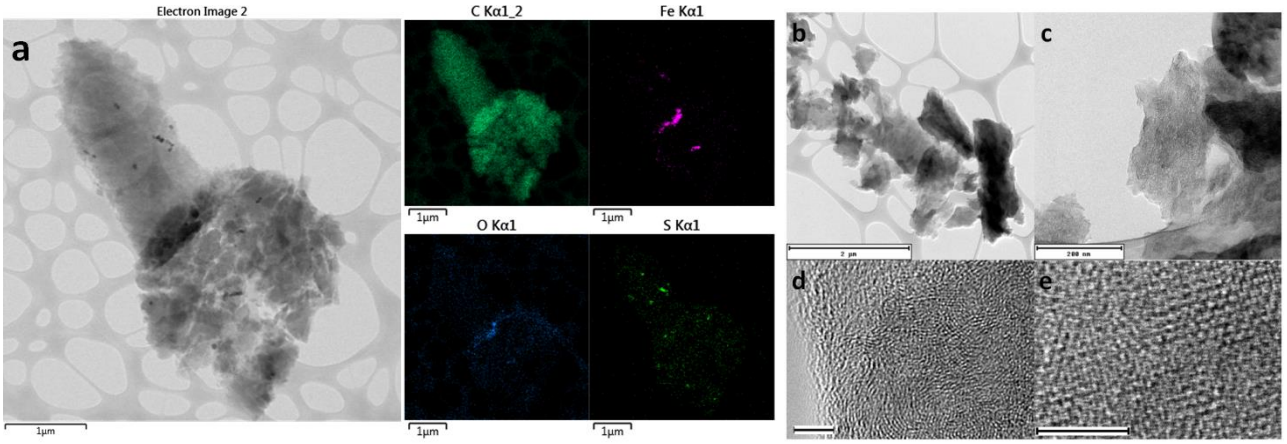

Figure 3. The elemental distribution map and corresponding TEM image (a). Scale bars corresponds to 1 μm. The TEM images of shungite particles (b and c) and HR-TEM images (d and e). The scale bars correspond to 2 μm and 0.2 μm (b and c) and to 5 nm (d and e).

Figure 2d shows the high resolution XPS spectrum of the C 1s core levels for shungite which brings further insight to the chemical composition of the oxygen-containing groups. The spectrum showed a double peak profile at 284.5 and 286.5 eV, the later with an asymmetrical tail at higher energies. The C 1s spectra were deconvoluted into five peaks, with the sp^2 hybridized carbon (C=C) at 284.4 eV, the sp^3 hybridized carbon (C-C) at 285.5 eV, the alcohol and ether groups (C-O) at 286.5 eV, the carbonyl group (C=O) group at 287.7 eV and carboxyl groups (O-C=O) at 290.1 eV. From the deconvolution (Table S1) the relative abundance of C-O groups is the highest with 40%, followed by C=O and O-C=O groups with

10.1002/chem.201703974

around 9%. This result points that shungite is a carbon material with high concentration of oxygen functionalities which are known to also have an impact in electrochemical sensing applications.[21]

Chemical composition of shungite was also studied by ICP-MS (Table 1), which further reveals a heterogeneous matrix loaded with different classes of elements, with Al and Ga (group 13) having the highest concentration. Several transitional metals and alkaline earth metals were also detected. It should be emphasized that the detection of some acute toxic elements, Pb and As at mg/g level, which have to be addressed before considering day-to-day applications of such material. The array of elements detected by EDX, XPS and ICP is not surprising. It is estimated that massive shungite containing rocks hold within its structural heterogeneity metal rich minerals such as sericite ($KAl_2(AlSi_3O_{10})(OH)_2$), calcite ($CaCO_3$), chlorite ($A_{5\text{-}6}T_4Z_{18}$, where A= Al, Fe, Li, Mg, Mn, or Ni, while T= Al, Fe, Si, or a combination of them, and Z= O and/or OH) or feldspar (metal silicates).[9]

Table 1. Metallic elements content in shungite samples as determined by inductively coupled plasma mass spectrometry analysis.

Element	Al	Ga	Li	Sb	Ba	Pb	Fe	Be	K	Rb	Mg	Sr	Sn	As	Zn, Na	Cr, Ni, Ca,Cs	Cu, Bi, Ti, V, Se
mg/g	131.7	41.9	27.3	19.0	13.2	6.7	5.0	3.5	3.1	1.3	1.1	0.8	0.7	0.4	0.3	0.2	0.1

Electrochemistry. Electrochemical fundamental studies of shungite in contrast with different carbon materials (C_{60}, CB and CNT) were subsequently performed. To probe electrochemical performance of modified GC electrodes with each carbon materials, cyclic voltammograms of an inner-sphere redox probe ferro/ferricyanide, $[Fe(CN)_6]^{3+/4+}$, were recorded in anodic direction (Figure 4a). Analyses of the voltammetric profiles were taken in terms of peak-to-peak potential (ΔE_p) of the oxidation and reduction processes, where a ΔE_p of 59 mV/e^- is the reversible limit, in which the smaller ΔE_p means the electrode performance is improved. The bare GC electrode has an average ΔE_p of 244 mV. This corresponds to an irreversible electron transfer process with little improvement at C_{60} and CNT modified electrode. Furthermore, it is noticeable that shungite has a much lower ΔE_p and comparable to CB (70 mV), thus having very good electron transfer properties.

10.1002/chem.201703974

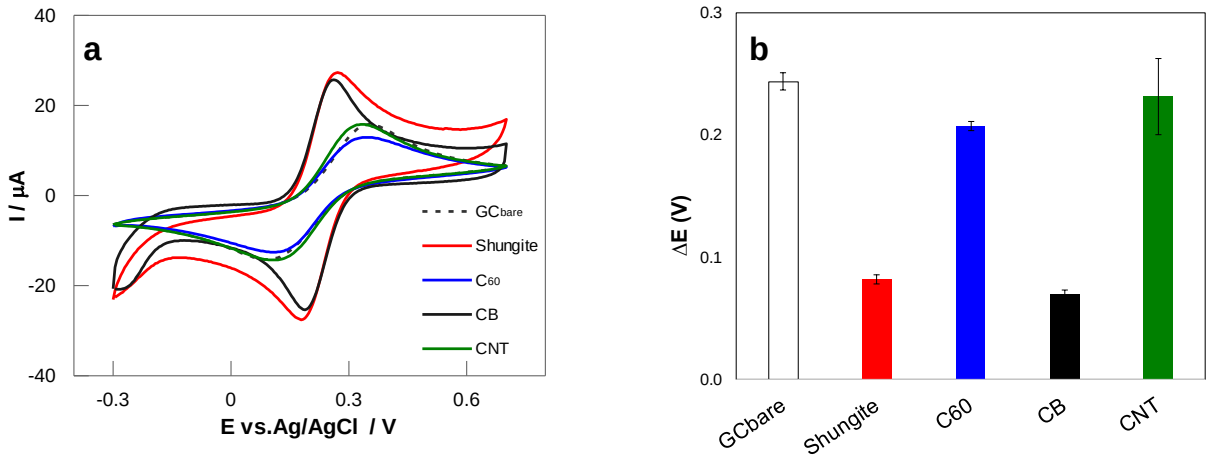

Figure 4. (a) Cyclic voltammograms obtained for 1.0 mM ferro/ferricyanide $[Fe(CN)_6]^{3+/4+}$redox probe in KCl 0.1 M for GC electrode and the different carbon materials. (b) Average peak-to-peak separation and standard deviation calculated from CVs. All voltammograms recorded at a scan rate of 100 mV/s.

Energy related applications. Energy related applications of shungite were also evaluated by testing their catalytic activity for the hydrogen evolution reaction (HER), oxygen evolution reaction (OER) and oxygen reduction reaction (ORR). Oxygen evolution reaction (OER) electrolysis represents an important half-reaction involved in water splitting with the application in rechargeable metal-air batteries mainly. This reaction has been intensely investigated for decades and lowest known overpotentials are obtained for the precious metal oxides IrO_2 and RuO_2.[22] The polarization curves performed in alkaline media are shown in Figure 5a. The best catalytic performance is clearly observed for shungite with an onset potential of +1.09 V vs. RHE for a 10 mA/cm^{-2}. The remain of the carbon materials exhibited higher OER onset potentials, almost indistinct form the bare GC electrode (+1.80 V vs. RHE). In the case of shungite, the rich combination of several transitional metals (Table 1), alkaline earth metals (Be, Mg and Sr), but most importantly group 13 elements (Al and Ga in the highest concentrations) in the carbon matrix structure has a catalytic effect in the OER. Shungite and carbon materials were also tested for oxygen reduction reaction (ORR) as displayed in Figure S9. ORR peaks yielded similar potentials of the GC_{bare} electrode, which means that in this case the reaction is not significantly catalyzed.

HER is a cathodic half reaction of water splitting and the applications of energy conversion devices including water electrolysis and artificial photosynthetic cells. Noble metals, such as Pt, show highest efficiency for HER. The HER polarization curves of shungite and other carbon materials in acidic media with the respective summary of the onset potentials at -10

mA/cm^{-2} are presented in Figure 5a and b. HER measurements of bare GC_{bare} (-1.48 V vs RHE) and Pt (-0.16 V vs RHE) are also shown as performance references. The metallic elements in present in shungite matrix as shown in Table 1, are in their majority base metals (Fe, Pb, Ni, Cu and Zn) that oxidize in acid media to form H_2.[23] Shungite has therefore improved HER catalytic performance with respect to other carbon materials, even the "catalytic" CNT.

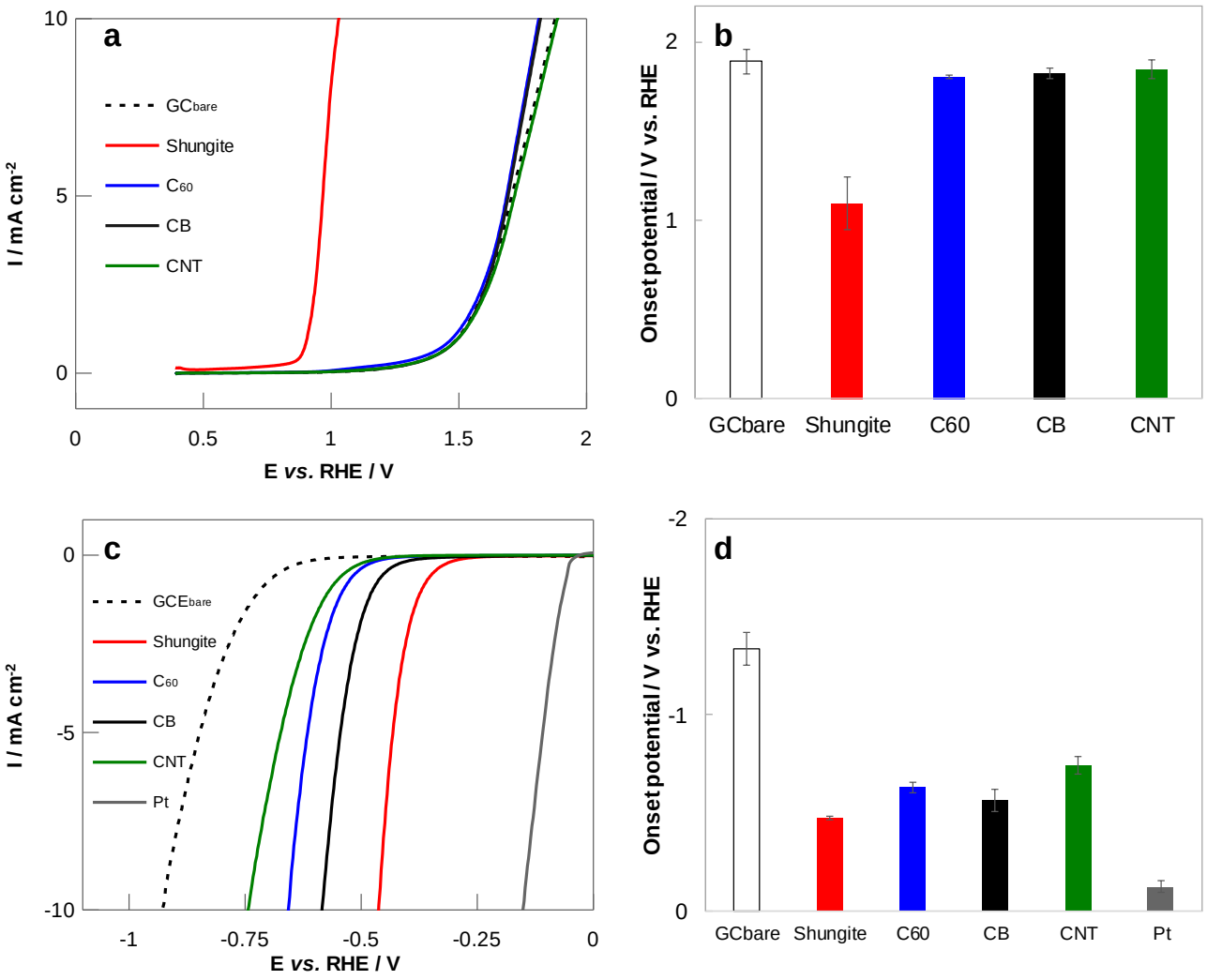

Figure 5. LSV corresponding to OER and HER in 1.0 M KOH (a) and 0.5 M H_2SO_4 (c) for the set of carbon materials with the corresponding average of the overpotential at a current density of +/-10 mA /cm^2 (b and d). Error bars correspond to standard deviations based on triplicate measurements. Scan rate: 5 mV/s.

Conclusions

Shungite reveals itself to be a complex raw carbon matrix, loaded a wide range of metallic elements at the mg/g level. The different classes of elements contribute for shungite as an interesting carbocatalyst in a different range of electrochemical reactions, outperforming other tested "catalytic" carbon materials (carbon black, carbon nanotubes, fullerene and glassy carbon).

Such results are in line with reported metal-doped carbon materials exhibiting enhanced electrocatalysis.[24] On the other hand, the presence of metallic impurities in "pure" carbon materials have sometimes misled to an incorrect credit of CNT and graphene as being "metal-free" catalysts due to their inherent properties.[25,26] Sources of such impurities usually lies on the purity starting carbon materials[27] and origins,[28] as well as, contaminations that come in contact with the material along the exfoliation or purification processes.[29] Herein we have used shungite without any purification, controlling the presence of other elements and how they enhance its electrochemical performance.

Methods

Reagents. Shungite was obtained from Shunga district, Karelia, Russia. Other carbon allotropes, carbon black (CB, mesoporous, average pore ϕ 100 ±10 Å), multiwalled carbon nanotubes (CNT, ϕ=110-170 nm, *l*=5-9 μm) and fullerene (Buckminsterfullerene, C_{60}) were obtained from Sigma-Aldrich. N,N-dimethylformamide (DMF), potassium ferrocyanide, potassium chloride, potassium hydroxide, potassium phosphate dibasic, potassium phosphate monobasic, potassium chloride and sulphuric acid were purchased from Sigma Aldrich.

Structural and morphological characterization. Prior to proceeding with the shungite studies, the acquired rock of several cm wide was smashed into smaller fragments which were further grinded for a few seconds using a kitchen blender as shown and detailed in Figure S10. To obtain SEM micrographs, scanning electron microscopy (JEOL 7600F, Japan) was used, at an acceleration voltage of 5 kV. The materials investigated were affixed on an aluminium sample stub using conductive carbon tape for imaging. EDS measurements were conducted at a higher acceleration voltage of 15 kV. The XPS spectra were obtained using X-ray photoelectron Phoibos 100 MCD-5 spectrometer (SPECS, Germany) with a monochromatic Mg Kα radiation (SPECS XR50, $h\upsilon$ = 1253 eV, 200 W) as the X-ray source, the spectra were calibrated to the C 1s peak at 284.5 eV. InVia Raman microscope (Renishaw, England) was used for Raman spectroscopy measurements in backscattering geometry with a CCD detector. Nd:YAG laser (514 nm, 50 mW) and 100x objectives were used for the measurement. The instrument calibration was achieved using a silicon reference which gave the peak position at 520 cm^{-1} and a resolution of less than 1 cm^{-1}. To ensure a sufficiently strong signal and to avoid radiation damage to the samples, the laser power used for these

measurements was 5 mW. X-ray powder diffraction data were collected at room temperature on Bruker D8 Discoverer powder diffractometer with parafocusing Bragg–Brentano geometry using CuKα radiation (λ = 0.15418 nm, U = 40 kV, I = 40 mA). Data were scanned over the angular range 5–90° (2θ) with a step size of 0.019° (2θ). Data evaluation was performed in the software package EVA. Transmission electron microscopy images were obtained using EFTEM Jeol 2200 FS microscope. Sample was prepared by drop casting of sample suspension (1 mg/mL) on 200 mesh TEM grid. Elemental maps and EDS spectra were enquired with SDD detector X-MaxN 80 T S from Oxford Instruments (England).

Chemical composition. Sample has been prepared using microwave assisted acid digestion (Milestone ETHOS 1, Italy) for inductively coupled plasma mass spectrometery (ICP-MS, Agilent 7700, Japan) analysis. Prior analysis, ICP-MS calibrated using mixture standard of 60 elements making from single standards.

***Electrochemical Measurements*.** Electrochemical measurements were carried out at room temperature using an Autolab PGSTAT204 (Eco Chemie, Utrecht, The Netherlands) controlled by NOVA Version 2.1 software (Eco Chemie) and three electrodes arrangement. Glassy carbon GC electrode (3 mm diameter from CH Instruments, Texas, USA) was used as a working electrode, Pt as counter electrode and Ag/AgCl as reference electrode (2 mm diameter from CH Instruments, Texas, USA). Each material was dispersed in DMF at a concentration of 5 mg/mL and sonicated initially for 15 minutes in an ultrasonic ice bath (T< 20 ºC). Prior to GC modification, each suspension was mechanically stirred for 1 minute using a vortex. Working electrode modification was done by drop casting 2 µL of each suspension.

Solutions were purged with nitrogen gas before measurements. The heterogeneous electron transfer (HET) rates measurements were done at a scan rate of 0.1 V/s, for 1.0 mM of the ferro/ferricyanide redox probe in a 0.1 M KCl solution.

The hydrogen evolution reaction (HER), oxygen reaction reduction (ORR) and oxygen evolution reaction (OER) were performed by linear sweep voltammetry (LSV) at a scan rate of 0.005 V/s. The HER was performed in 0.5 M H_2SO_4 (acidic media) and 1.0 M KOH (alkaline media), while ORR and OER were done exclusively in alkaline media.

References

[1] H. W. Kroto, J. R. Heath, S. C. O'Brien, R. F. Curl, R. E. Smalley, *Nature* **1985**, *318*, 162–163.

[2] P. R. Buseck, S. J. Tsipursky, R. Hettich, *Science (80-.).* **1992**, *257*, 215–217.

[3] Y. Gu, M. A. Wilson, K. J. Fisher, I. G. Dance, G. D. Willett, D. Ren, I. B. Volkova, *Carbon N. Y.* **1995**, *33*, 862–863.

[4] D. Heymann, *Carbon N. Y.* **1995**, *33*, 237–239.

[5] R. L. Hettich, P. R. Buseck, *Carbon N. Y.* **1996**, *34*, 685–687.

[6] E. V. Osipov, V. A. Reznikov, *Carbon N. Y.* **2002**, *40*, 961–965.

[7] V. V. Kovalevski, P. R. Buseck, J. M. Cowley, *Carbon N. Y.* **2001**, *39*, 243–256.

[8] V. A. Melezhik, A. E. Fallick, M. M. Filippov, O. Larsen, *Karelian Shungite-an Indication of 2.0-Ga-Old Metamorphosed Oil-Shale and Generation of Petroleum: Geology, Lithology and Geochemistry*, **1999**.

[9] V. A. Melezhik, M. M. Filippov, A. E. Romashkin, *Ore Geol. Rev.* **2004**, *24*, 135–154.

[10] J. Jehlička, O. Frank, V. Hamplová, Z. Pokorná, L. Juha, Z. Boháček, Z. Weishauptová,

Carbon N. Y. **2005**, *43*, 1909–1917.
[11] S. Iijima, *Nature* **1991**, *354*, 56–58.
[12] L. V. Radushkevich, V. M. Lukyanovich, *Zurn Fis. Chim* **1952**, *26*, 88–95.
[13] M. Monthioux, V. L. Kuznetsov, *Carbon N. Y.* **2006**, *44*, 1621–1623.
[14] A. K. Geim, K. S. Novoselov, *Nat Mater* **2007**, *6*, 183–191.
[15] B. C. Brodie, *Philos. Trans. R. Soc. London* **1859**, *149*, 249–259.
[16] A. Carvalho, M. Wang, X. Zhu, A. S. Rodin, H. Su, A. H. Castro Neto, *Nat. Rev. Mater.* **2016**, *1*, 16061.
[17] X. Chia, A. Y. S. Eng, A. Ambrosi, S. M. Tan, M. Pumera, *Chem. Rev.* **2015**, *115*, 11941–11966.
[18] K. S. Novoselov, A. Mishchenko, A. Carvalho, A. H. Castro Neto, *Science* **2016**, *353*, aac9439-aac9439.
[19] R. Gusmão, Z. Sofer, M. Pumera, *Angew. Chemie Int. Ed.* **2017**, *56*, 8052–8072.
[20] G. Khavari-Khorasani, D. G. Murchison, *Chem. Geol.* **1979**, *26*, 165–182.
[21] R. Gusmão, V. López-Puente, I. Pastoriza-Santos, J. Pérez-Juste, M. F. Proença, F. Bento, D. Geraldo, M. C. Paiva, E. González-Romero, *RSC Adv.* **2015**, *5*, 5024–5031.
[22] N.-T. Suen, S.-F. Hung, Q. Quan, N. Zhang, Y.-J. Xu, H. M. Chen, *Chem. Soc. Rev.* **2017**, *46*, 337–365.
[23] R. Gusmão, Z. Sofer, M. Nováček, J. Luxa, S. Matějková, M. Pumera, *Nanoscale* **2016**, *8*, 6700–6711.
[24] A. Ambrosi, C. K. Chua, N. M. Latiff, A. H. Loo, C. H. A. Wong, A. Y. S. Eng, A. Bonanni, M. Pumera, *Chem. Soc. Rev.* **2016**, *45*, 2458–2493.
[25] M. Pumera, *Langmuir* **2007**, *23*, 6453–6458.
[26] C. E. Banks, A. Crossley, C. Salter, S. J. Wilkins, R. G. Compton, *Angew. Chemie Int. Ed.* **2006**, *45*, 2533–2537.
[27] A. Ambrosi, C. K. Chua, B. Khezri, Z. Sofer, R. D. Webster, M. Pumera, *Proc. Natl. Acad. Sci.* **2012**, *109*, 12899–12904.
[28] C. H. A. Wong, Z. Sofer, M. Pumera, *Chem. - A Eur. J.* **2015**, *21*, 8435–8440.
[29] C. H. A. Wong, Z. Sofer, M. Kubesova, J. Kucera, S. Matejkova, M. Pumera, *Proc. Natl. Acad. Sci.* **2014**, *111*, 13774–13779.

Acknowledgements

M.P. was funded by Tier 1 (01/13) from Ministry of Education, Singapore. Z. S. and D. B. were supported by Czech science foundation (GACR No. 15-09001S and GACR No. 16-05167S) and by specific university research (MSMT No. 20-SVV/2017). This work was created with the financial support of the Neuron Foundation for science support. The authors also acknowledge Dr. B. Khezri her assistance with the ICP-MS results.

Supporting Information accompanies this paper.

10.1002/chem.201703974

Competing financial interests: The authors declare no competing financial interests.

10.1002/chem.201703974

Image for Table of Contents

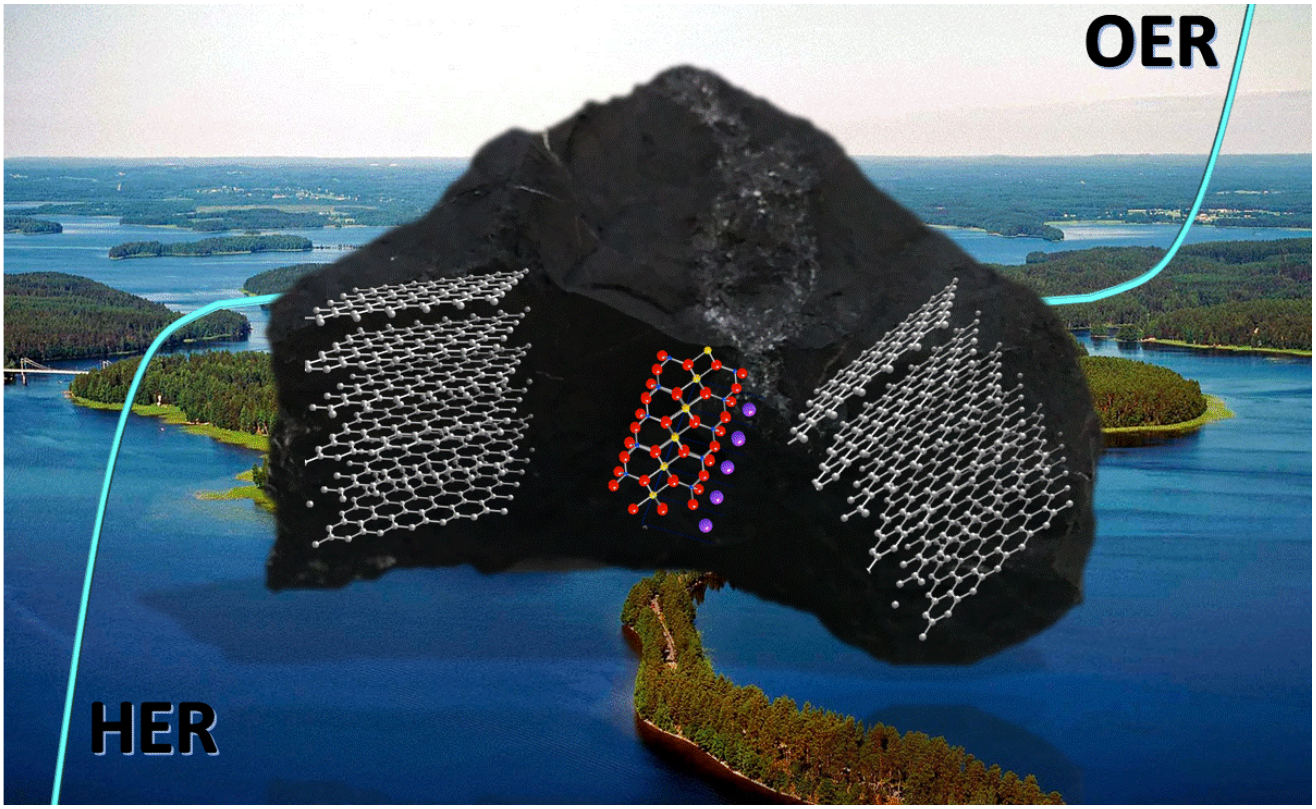

TOC capture: Shungite is carbon rock from Lake Onega, Karelia (Russia) with a heterogeneous molecular structure rich in carbon that may contain within its structure metal rich minerals (*e.g.*: sericite). Metallic elements detected in shungite matrix were found to have a synergetic effect in the catalytic performance towards HER and OER.